REPORT DOCUMENTATION PAGE

Form Approved OMB NO. 0704-0188

1. REPORT DATE (DD-MM-YYYY)	2. REPORT TYPE	3. DATES COVERED (From - To)
17-05-2022	Final Report	15-Jan-2019 - 14-Jan-2021

4. TITLE AND SUBTITLE
Final Report: New Principles for Targeting and Triggering based on Molecular Self-Assembly in Topological Defects of Liquid Crystals

5a. CONTRACT NUMBER
W911NF-19-1-0071

5b. GRANT NUMBER

5c. PROGRAM ELEMENT NUMBER
611102

6. AUTHORS

5d. PROJECT NUMBER

5e. TASK NUMBER

5f. WORK UNIT NUMBER

7. PERFORMING ORGANIZATION NAMES AND ADDRESSES
Cornell University
Office of Sponsored Programs
373 Pine Tree Road
Ithaca, NY 14850 -2820

8. PERFORMING ORGANIZATION REPORT NUMBER

9. SPONSORING/MONITORING AGENCY NAME(S) AND ADDRESS (ES)
U.S. Army Research Office
P.O. Box 12211
Research Triangle Park, NC 27709-2211

10. SPONSOR/MONITOR'S ACRONYM(S)
ARO

11. SPONSOR/MONITOR'S REPORT NUMBER(S)
74817-CH.20

12. DISTRIBUTION AVAILIBILITY STATEMENT
Approved for public release; distribution is unlimited.

13. SUPPLEMENTARY NOTES
The views, opinions and/or findings contained in this report are those of the author(s) and should not contrued as an official Department of the Army position, policy or decision, unless so designated by other documentation.

14. ABSTRACT

15. SUBJECT TERMS

16. SECURITY CLASSIFICATION OF:			17. LIMITATION OF ABSTRACT	15. NUMBER OF PAGES	19a. NAME OF RESPONSIBLE PERSON
a. REPORT	b. ABSTRACT	c. THIS PAGE			Nicholas Abbott
UU	UU	UU	UU		19b. TELEPHONE NUMBER 607-255-3601

RPPR Final Report
as of 06-Jun-2022

Agency Code: 21XD

Proposal Number: 74817CH **Agreement Number: W911NF-19-1-0071**
INVESTIGATOR(S):

Name: Nathan Gianneschi
Email: nathan.gianneschi@northwestern.edu
Phone Number: 8474672013
Principal: N

Name: Nicholas Abbott
Email: nla34@cornell.edu
Phone Number: 6072553601
Principal: Y

Organization: **Cornell University**
Address: Office of Sponsored Programs, Ithaca, NY 148502820
Country: USA
DUNS Number: 872612445 EIN: 150532082

Report Date: 14-Apr-2021 Date Received: 17-May-2022
Final Report for Period Beginning 15-Jan-2019 and Ending 14-Jan-2021

Title: New Principles for Targeting and Triggering based on Molecular Self-Assembly in Topological Defects of Liquid Crystals
Begin Performance Period: 15-Jan-2019 **End Performance Period:** 14-Jan-2021
Report Term: 0-Other

Submitted By: Nicholas Abbott Email: nla34@cornell.edu
Phone: (607) 255-3601

Distribution Statement: 1-Approved for public release; distribution is unlimited.

STEM Degrees: 2 **STEM Participants:** 3

Major Goals: This project was focused on understanding equilibrium and dynamic aspects of molecular self-assembly of amphiphiles and polymers in defects of nematic solvents, and leveraging that understanding to demonstrate new principles that permit formation and manipulation of single nanoscopic assemblies. The approach built from Abbott's discovery that molecular assemblies can be formed in topological defects of liquid crystals. A particular focus of this collaborative research project between the Abbott and Gianneschi groups was directed to development of structure-property relationships for self-assembly of polymers in topological defects of liquid crystals. The efforts aimed to generate a number of important advances, including the use of RAFT to synthesize homopolymers and copolymers for development of structure-property relationships, including self-assembly in bulk LCs and defects of LCs. A second focus of the proposal revolved around the manipulation of defects in LCs using electric fields. Specifically, we aimed to demonstrate control of the formation and disassembly of single polymeric and amphiphilic assemblies, by using electric fields to relocate defects to areas of LC that contain targeted polymers or amphiphiles. Overall, the research aimed to use of topological defects as nanoscopic reactors that can host both chemical and physical transformations, and be readily manipulated to add and remove reagents.

Accomplishments: Please see the attached PDF

Training Opportunities: This project provided outstanding training opportunities for graduate students and postdoctoral researchers to participate in multi-disciplinary and multi-institutional research. Regular teleconferences and in-person discussions provide graduate students in chemical engineering with the opportunity to work with postdoctoral researchers from chemistry. Undergraduate researchers were also integrated into both research groups, providing opportunities for undergraduates to understand the purposes and processes of research.

RPPR Final Report
as of 06-Jun-2022

Results Dissemination: The PIs have given a range of presentations on their ARO-supported research, including in-person talks at conferences and workshops as well as virtual presentations due to COVID-19. For example, Abbott gave two talks at the ACS Colloid and Surface Chemistry symposium held in March 2020, and he gave an institute colloquium to the Liquid Crystal Institute at Kent State University in May of 2020. He was scheduled to give four invited talks in Europe over the summer of 2021 but they were postponed due to restrictions on travel. Other examples of talks given by Abbott are summarized below

San Diego, keynote lecture at 22nd Liquid Crystal Conference [LCXXII], held in conjunction with the 2018

SPIE Annual Symposium on Optics and Photonics.

Ankara, Turkey, Middle East Technical University, invited talk at 60th Anniversary of Chemical Engineering at METU.

Ljubjana, Slovenia, European Colloid and Interface Science Conference, invited talk in Satellite Session on Colloid Science and Chemical Engineering

Tokyo, Japan, Plenary Lecture for the Division of Colloid and Surface Chemistry, Chemical Society of Japan.

Tokyo, Japan, Tokyo University of Science, seminar in the Department of Chemistry.

Pittsburgh, Annual Meeting of American Institute of Chemical Engineers, talk in session on Self-Assembly in Solution.

Pittsburgh, Annual Meeting of American Institute of Chemical Engineers, invited talk at Symposium on New Frontiers on Molecular Thermodynamics.

Pittsburgh, Annual Meeting of American Institute of Chemical Engineers, invited talk at Symposium to Honor Jacques Zakin.

Changshu, China, United World College, Outreach seminar on liquid crystals to high school students.

Natick, MA, Natick Soldier Research, Development, & Engineering Center, invited talk at Antimicrobial Textiles Colloquium.

Kanpur, India, invited talk at IUTAM Symposium on Dynamics of Complex Fluids and Interfaces.

Honors and Awards: Honors to Abbott include

2022 John Quinn Lecture, University of Pennsylvania
2021 Plenary Lecture, Liquid Matter Conference
2019 Rockwell Lecture, Department of Chemical Engineering, University of Houston.
2018 Lectureship Award of Division of Colloid and Surface Chemistry, Chemical Society of Japan.
2018 Tisch University Professor, Smith School of Chemical and Biomolecular Engineering, Cornell University
2018 Patten Distinguished Lecture, University of Colorado-Boulder
2018 Reilly Lectures, University of Notre Dame
2017 6th Somer Lectures, Middle East Technical University, Ankara, Turkey.

Protocol Activity Status:

Technology Transfer: Abbott reviewed proposals at the request of Kathleen Swana, CCDC Soldier Center, Natick MA.

October, 2018. Abbott visited Natick to participate in a workshop on novel strategies for delivery of antimicrobial treatments. Workshop was organized by Molly (Clay) Richards. Presented work on triggered release of antimicrobial gases and antimicrobial salts. Follow up discussions occurred with Chris Doona.

February, 2019. Abbott participated in an ARO-sponsored workshop on "Materials that Compute", organized by Dr Anna Balazs, and held in Durham, NC.

PARTICIPANTS:

Participant Type: Co PD/PI
Participant: Nathan Gianneschi
Person Months Worked: 1.00 **Funding Support:**
Project Contribution:
National Academy Member: N

Participant Type: PD/PI
Participant: nicholas abbott
Person Months Worked: 1.00 **Funding Support:**
Project Contribution:
National Academy Member: Y

Participant Type: Postdoctoral (scholar, fellow or other postdoctoral position)
Participant: Wei cao
Person Months Worked: 12.00 **Funding Support:**
Project Contribution:
National Academy Member: N

Participant Type: Postdoctoral (scholar, fellow or other postdoctoral position)
Participant: Junghyun Noh
Person Months Worked: 12.00 **Funding Support:**
Project Contribution:
National Academy Member: N

Participant Type: Postdoctoral (scholar, fellow or other postdoctoral position)
Participant: Hao Sun
Person Months Worked: 12.00 **Funding Support:**
Project Contribution:
National Academy Member: N

ARTICLES:

RPPR Final Report
as of 06-Jun-2022

Publication Type: Journal Article Peer Reviewed: Y **Publication Status:** 1-Published
Journal: Langmuir
Publication Identifier Type: DOI Publication Identifier: 10.1021/acs.langmuir.8b03287
Volume: 35 Issue: 6 First Page #: 2078
Date Submitted: 5/20/19 12:00AM Date Published: 1/1/19 12:00AM
Publication Location:
Article Title: Molecular Order Affects Interfacial Water Structure and Temperature-Dependent Hydrophobic Interactions between Nonpolar Self-Assembled Monolayers
Authors: Bradley C. Dallin, Hongseung Yeon, Alexis R. Ostwalt, Nicholas L. Abbott, Reid C. Van Lehn
Keywords: DRIVING-FORCE; SURFACE-AREA; DYNAMICS; SOLVATION; LENGTH; GOLD; THERMODYNAMICS; NANOPARTICLES; SPECTROSCOPY; DIMERIZATION
Abstract: Understanding how material properties affect hydrophobic interactions-the water-mediated interactions that drive the association of nonpolar materials-is vital to the design of materials in contact with water. Conventionally, the magnitude of the hydrophobic interactions between extended interfaces is attributed to interfacial chemical properties, such as the amount of nonpolar solvent-exposed surface area. However, recent experiments have demonstrated that the hydrophobic interactions between uniformly nonpolar self-assembled monolayers (SAMs) also depend on molecular-level SAM order. In this work, we use atomistic molecular dynamics simulations to investigate the relationship between SAM order, water structure, and hydrophobic interactions to explain these experimental observations. The SAM-SAM hydrophobic interactions calculated from the simulations increase in magnitude as SAM order increases, matching experimental observations. We explain this trend by showing that the molecular-
Distribution Statement: 3-Distribution authorized to U.S. Government Agencies and their contractors
Acknowledged Federal Support: **Y**

Publication Type: Journal Article Peer Reviewed: Y **Publication Status:** 1-Published
Journal: Liquid Crystals
Publication Identifier Type: DOI Publication Identifier: 10.1080/02678292.2018.1509389
Volume: 45 Issue: First Page #: 2253
Date Submitted: 5/20/19 12:00AM Date Published: 8/1/18 12:00AM
Publication Location:
Article Title: Phosphorylation status of peptide monolayers modulates hydrogen bonding and orientations of nematic liquid crystals
Authors: Reza Abbasi, Chenxuan Wang, Yiqun Bai, Nicholas L. Abbott
Keywords: Thermotropic liquid crystals; oligopeptides; surface ordering; phosphorylation; hydrogen bonding
Abstract: We report on the azimuthal orientations of nematic liquid crystals (LCs) on monolayers of dipeptides and tripeptides containing cysteine (C) and either tyrosine (Y), serine (S) or threonine (T). Measurements performed with 5CB and TL205 (with and without doping with trimethylamine), and dipeptide monolayers in which we removed the -OH groups of CY, CS or CT, led us to conclude that hydrogen bonding strongly influences LC orientations on CY but not CS or CT monolayers. Chemical force microscopy and cyclic voltammetry support the hypothesis that intra-monolayer hydrogen bonding within monolayers of CS and CT occurs preferentially to hydrogen bonding with 5CB. In contrast, the orientations of the LCs on tripeptide monolayers of CAY, CAS or CAT, where A is alanine, were all influenced by hydrogen bonding, consistent with a decrease in surface density of tripeptides (as compared to dipeptides; supported by x-ray photoelectron spectroscopy) and increase in hydrogen bonding with the LC overla
Distribution Statement: 3-Distribution authorized to U.S. Government Agencies and their contractors
Acknowledged Federal Support: **Y**

RPPR Final Report
as of 06-Jun-2022

Publication Type: Journal Article Peer Reviewed: Y **Publication Status:** 1-Published
Journal: Science
Publication Identifier Type: DOI Publication Identifier: 10.1126/science.aar8449
Volume: 362 Issue: 6416 First Page #: 804
Date Submitted: 5/20/19 12:00AM Date Published: 11/1/18 12:00AM
Publication Location:
Article Title: Templated nanofiber synthesis via chemical vapor polymerization into liquid crystalline films
Authors: Kenneth C. K. Cheng, Marco A. Bedolla-Pantoja, Young-Ki Kim, Jason V. Gregory, Fan Xie, Alexander
Keywords: DEPOSITION; TRANSITION; SURFACES
Abstract: Extrusion, electrospinning, and microdrawing are widely used to create fibrous polymer mats, but these approaches offer limited access to oriented arrays of nanometer-scale fibers with controlled size, shape, and lateral organization. We show that chemical vapor polymerization can be performed on surfaces coated with thin films of liquid crystals to synthesize organized assemblies of end-attached polymer nanofibers. The process uses low concentrations of radical monomers formed initially in the vapor phase and then diffused into the liquid-crystal template. This minimizes monomer-induced changes to the liquid-crystal phase and enables access to nanofiber arrays with complex yet precisely defined structures and compositions. The nanofiber arrays permit tailoring of a wide range of functional properties, including adhesion that depends on nanofiber chirality.
Distribution Statement: 3-Distribution authorized to U.S. Government Agencies and their contractors
Acknowledged Federal Support: **Y**

Publication Type: Journal Article Peer Reviewed: Y **Publication Status:** 1-Published
Journal: Langmuir
Publication Identifier Type: DOI Publication Identifier: 10.1021/acs.langmuir.8b01944
Volume: 34 Issue: 34 First Page #: 10092
Date Submitted: 5/20/19 12:00AM Date Published: 7/1/18 4:00AM
Publication Location:
Article Title: Oligomers as Triggers for Responsive Liquid Crystals
Authors: Young-Ki Kim, Krishna R. Raghupathi, Joel S. Pendery, Piyachai Khomein, Uma Sridhar, Juan J. de Pa
Keywords: NEMATIC-ISOTROPIC INTERFACE; POLYMER MATERIALS; DROPLETS; ASSEMBLIES; DESIGN; MICROFLUIDICS; NANOCARRIERS; AMPHIPHILES; BIOSENSOR; ALIGNMENT
Abstract: We report an investigation of the influence of aqueous solutions of amphiphilic oligomers on the ordering of micrometer-thick films of thermotropic liquid crystals (LCs), thus addressing the gap in knowledge arising from previous studies of the interactions of monomeric and polymeric amphiphiles with LCs. Specifically, we synthesized amphiphilic oligomers (with decyl hydrophobic and pentaethylene glycol hydrophilic domains) in monomer, dimer, and trimer forms, and incubated aqueous solutions of the oligomers against nematic films of 4'-pentyl-4-biphenylcarbonitrile (5CB). All amphiphilic oligomers caused sequential surface-driven orientational (planar to homeotropic) and then bulk phase transitions (nematic to isotropic) with dynamics depending strongly on the degree of oligomerization. The dynamics of the orientational transitions accelerated from monomer to trimer, consistent with the effects of an increase in adsorption free energy. The mechanism underlying the orientational transit
Distribution Statement: 3-Distribution authorized to U.S. Government Agencies and their contractors
Acknowledged Federal Support: **Y**

RPPR Final Report
as of 06-Jun-2022

Publication Type: Journal Article Peer Reviewed: Y **Publication Status:** 1-Published
Journal: ChemPhysChem
Publication Identifier Type: DOI Publication Identifier: 10.1002/cphc.201800106
Volume: 19 Issue: 16 First Page #: 2037
Date Submitted: 5/20/19 12:00AM Date Published: 8/1/18 4:00AM
Publication Location:
Article Title: Multi-Scale Responses of Liquid Crystals Triggered by Interfacial Assemblies of Cleavable Homopolymers
Authors: Young-Ki Kim, Yuran Huang, Michael Tsuei, Xin Wang, Nathan C. Gianneschi, Nicholas L. Abbott
Keywords: cleavable homopolymers; liquid crystals; smart materials; stimuli-responsive materials; triggering
Abstract: Liquid crystals (LCs) offer the basis of stimuli-responsive materials that can amplify targeted molecular events into macroscopic outputs. However, general and versatile design principles are needed to realize the full potential of these materials. To this end, we report the synthesis of two homopolymers with mesogenic side chains that can be cleaved upon exposure to either H2O2 (polymer P1) or UV light (polymer P2). Optical measurements reveal that the polymers dissolve in bulk LC and spontaneously assemble at nematic LC-aqueous interfaces to impose a perpendicular orientation on the LCs. Subsequent addition of H2O2 to the aqueous phase or exposure of the LC to UV was shown to trigger a surface-driven ordering transition to a planar orientation and an accompanying macroscopic optical output. Differences in the dynamics of the response to each stimulus are consistent with sequential processing of P1 at the LC-aqueous interface (H2O2) and simultaneous transformation of P2 within the LC
Distribution Statement: 3-Distribution authorized to U.S. Government Agencies and their contractors
Acknowledged Federal Support: **Y**

Publication Type: Journal Article Peer Reviewed: Y **Publication Status:** 1-Published
Journal: Angewandte Chemie International Edition
Publication Identifier Type: DOI Publication Identifier: 10.1002/anie.201803194
Volume: 57 Issue: 31 First Page #: 9665
Date Submitted: 5/20/19 12:00AM Date Published: 7/1/18 12:00AM
Publication Location:
Article Title: Redox-Triggered Orientational Responses of Liquid Crystals to Chlorine Gas
Authors: Tibor Szilvási, Nanqi Bao, Karthik Nayani, Huaizhe Yu, Prabin Rai, Robert J. Twieg, Manos Mavrikakis,
Keywords: anchoring transitions; Cl-2 detection; liquid crystals; redox chemistry; sensors
Abstract: Surface-supported liquid crystals (LCs) that exhibit orientational and thus optical responses upon exposure to ppb concentrations of Cl-2 gas are reported. Computations identified Mn cations as candidate surface binding sites that undergo redox-triggered changes in the strength of binding to nitrogen-based LCs upon exposure to Cl-2 gas. Guided by these predictions, m-thick films of nitrile- or pyridine-containing LCs were prepared on surfaces decorated with Mn2+ binding sites as perchlorate salts. Following exposure to Cl-2, formation of Mn4+ (in the form of MnO2 microparticles) was confirmed and an accompanying change in the orientation and optical appearance of the supported LC films was measured. In unoptimized systems, the LC orientational transitions provided the sensitivity and response times needed for monitoring human exposure to Cl-2 gas. The response was also selective to Cl-2 over other oxidizing agents such as air or NO2 and other chemical targets such as organophosphonates
Distribution Statement: 3-Distribution authorized to U.S. Government Agencies and their contractors
Acknowledged Federal Support: **Y**

RPPR Final Report
as of 06-Jun-2022

Publication Type: Journal Article Peer Reviewed: Y **Publication Status:** 1-Published
Journal: Nature
Publication Identifier Type: DOI Publication Identifier: 10.1038/s41586-018-0098-y
Volume: 557 Issue: 7706 First Page #: 539
Date Submitted: 5/20/19 12:00AM Date Published: 5/1/18 12:00AM
Publication Location:
Article Title: Self-reporting and self-regulating liquid crystals
Authors: Young-Ki Kim, Xiaoguang Wang, Pranati Mondkar, Emre Bukusoglu, Nicholas L. Abbott
Keywords: INTERFACIAL-TENSION; DELIVERY-SYSTEMS; ISOTROPIC-PHASE; PARTICLES; DROPLETS; DESIGN; LAYER
Abstract: Liquid crystals (LCs) are anisotropic fluids that combine the long-range order of crystals with the mobility of liquids(1,2). This combination of properties has been widely used to create reconfigurable materials that optically report information about their environment, such as changes in electric fields (smart-phone displays) (3), temperature (thermometers)(4) or mechanical shear(5), and the arrival of chemical and biological stimuli (sensors)(6,7). An unmet need exists, however, for responsive materials that not only report their environment but also transform it through self-regulated chemical interactions. Here we show that a range of stimuli can trigger pulsatile (transient) or continuous release of microcargo (aqueous microdroplets or solid microparticles and their chemical contents) that is trapped initially within LCs. The resulting LC materials self-report and self-regulate their chemical response to targeted physical, chemical and biological events in ways that can be preprog
Distribution Statement: 3-Distribution authorized to U.S. Government Agencies and their contractors
Acknowledged Federal Support: **Y**

Publication Type: Journal Article Peer Reviewed: Y **Publication Status:** 1-Published
Journal: Soft Matter
Publication Identifier Type: Publication Identifier: DOI
Volume: 15 Issue: 35 First Page #:
Date Submitted: 5/17/22 12:00AM Date Published:
Publication Location:
Article Title: Soft Matter from Liquid Crystals
Authors: Young-Ki Kim,a,b JungHyun Noh,a Karthik Nayani,a and Nicholas L. Abbott
Keywords: liquid crystals, defects, self-assembly
Abstract: Mammalian cells are soft, and correct functioning requires that cells undergo dynamic shape changes in vivo. Although a range of diseases are associated with stiffening of red blood cells (RBCs; e.g., sickle cell anemia or malaria), the mechanical properties and thus shape responses of cells to complex viscoelastic environments are poorly understood. We use vapor pressure measurements to identify aqueous liquid crystals (LCs) that are in osmotic equilibrium with RBCs and explore mechanical coupling between RBCs and LCs. When transferred from an isotropic aqueous phase into a LC, RBCs exhibit complex yet reversible shape transformations, from initially biconcave disks to elongated and folded geometries with noncircular cross-sections. Importantly, whereas the shapes of RBCs are similar in isotropic fluids, when strained by LC, a large variance in shape response is measured, thus unmasking cell-to-cell variation in mechanical properties. Numerical modeling of LC and cell mechanics reveal
Distribution Statement: 2-Distribution Limited to U.S. Government agencies only; report contains proprietary info
Acknowledged Federal Support: **Y**

RPPR Final Report
as of 06-Jun-2022

Publication Type: Journal Article Peer Reviewed: Y **Publication Status:** 1-Published
Journal: Journal of American Chemical Society
Publication Identifier Type: Publication Identifier: 10.1021/jacs.9b08057
Volume: 141 Issue: 40 First Page #: 16003
Date Submitted: 8/31/20 12:00AM Date Published:
Publication Location:
Article Title: Amplification of Elementary Surface Reaction Steps on Tran-sition Metal Surfaces using Liquid Crystals: Dissociative Adsorption and Dehydrogenation
Authors: Huaizhe Yu, Tibor Szilva?si, Kunlun Wang, Jake I. Gold, Nanqi Bao, Robert J. Twieg, Manos Mavr
Keywords: liquid crystals, interfaces, self-assembly
Abstract: Aqueous-liquid crystal (LC) interfaces offer promise as respon-sive interfaces at which biomolecular recognition events can be amplified into macroscopic signals. However, the design of LC interfaces that distinguish between specific and non-specific protein interactions remains an unresolved challenge. Herein we report the synthesis of amphiphilic monomers, dimers and trimers conjugated to sulfonamide ligands via triazole rings, their assem-bly at aqueous-LC interfaces, and the orientational response of LCs to the interactions of carbonic anhydrase II (CAII) and serum albumin with the oligomer-decorated LC interfaces. Of six oli-gomers synthesized, only dimers without amide methylation were found to assemble at aqueous interfaces of nematic 4-cyano-4'-pentylbiphenyl (5CB) to induce perpendicular LC orientations. At dimer-decorated LC interfaces, we found that concentrations of CAII less than 4 ?M did not measurably perturb the LC but prevented....
Distribution Statement: 2-Distribution Limited to U.S. Government agencies only; report contains proprietary info
Acknowledged Federal Support: **Y**

Publication Type: Journal Article Peer Reviewed: Y **Publication Status:** 1-Published
Journal: Science Advances
Publication Identifier Type: DOI Publication Identifier: 10.1126/sciadv.abb1327
Volume: 6 Issue: 25 First Page #:
Date Submitted: 8/31/20 12:00AM Date Published: 6/1/20 4:00AM
Publication Location:
Article Title: Programming van der Waals interactions with complex symmetries into microparticles using liquid crystallinity
Authors: H. A. Fuster, Xin Wang, Xiaoguang Wang, E. Bukusoglu, S. E. Spagnolie, N. L. Abbott
Keywords: liquid crystals, assembly, van der Waals forces
Abstract: Van der Waals interactions dominate the organization of colloidal soft matter, leading to ubiquitous phenomena such as aggregation, crystallization, and gelation, and technologies such as paints, reflective films, and biological assays. Limited means exist, however, to control the symmetry of van der Waals interactions acting between colloids, even though past studies show that asymmetric interactions such as entropic forces (e.g., encoded by non-spherical shapes) and surface mediated forces (e.g., encoded by patterned surface chemistry) can provide access to new states of colloidal matter. Here we show that polymerization of liquid crystals (LCs) confined within microdroplets dispersed in water can be used to prepare compositionally homogeneous and spherical polymeric microparticles that encode van der Waals interactions with complex symmetries. We map the spatial variation of the van der Waals forces across the surfaces of the microparticles by kinetically-controlled adsorption
Distribution Statement: 2-Distribution Limited to U.S. Government agencies only; report contains proprietary info
Acknowledged Federal Support: **Y**

RPPR Final Report
as of 06-Jun-2022

Publication Type: Journal Article Peer Reviewed: Y **Publication Status:** 1-Published
Journal: Molecular Systems Design & Engineering
Publication Identifier Type: DOI Publication Identifier: 10.1039/D0ME00016G
Volume: 5 Issue: 4 First Page #: 835
Date Submitted: 5/17/22 12:00AM Date Published:
Publication Location:
Article Title: Influence of immobilized cations on the thermodynamic signature of hydrophobic interactions at chemically heterogeneous surfaces
Authors: Hongseung Yeon, Chenxuan Wang, Samuel H. Gellman, Nicholas L. Abbott
Keywords: self-assembly, hydrophobic interactions
Abstract: Mammalian cells are soft, and correct functioning requires that cells undergo dynamic shape changes in vivo. Although a range of diseases are associated with stiffening of red blood cells (RBCs; e.g., sickle cell anemia or malaria), the mechanical properties and thus shape responses of cells to complex viscoelastic environments are poorly understood. We use vapor pressure measurements to identify aqueous liquid crystals (LCs) that are in osmotic equilibrium with RBCs and explore mechanical coupling between RBCs and LCs. When transferred from an isotropic aqueous phase into a LC, RBCs exhibit complex yet reversible shape transformations, from initially biconcave disks to elongated and folded geometries with noncircular cross-sections. Importantly, whereas the shapes of RBCs are similar in isotropic fluids, when strained by LC, a large variance in shape response is measured, thus unmasking cell-to-cell variation in mechanical properties. Numerical modeling of LC and cell mechanics reveal
Distribution Statement: 2-Distribution Limited to U.S. Government agencies only; report contains proprietary info
Acknowledged Federal Support: **Y**

Publication Type: Journal Article Peer Reviewed: Y **Publication Status:** 1-Published
Journal: ACS Applied Materials & Interfaces
Publication Identifier Type: DOI Publication Identifier: 10.1021/acsami.9b16867
Volume: 12 Issue: 7 First Page #: 7869
Date Submitted: 8/31/20 12:00AM Date Published: 12/1/19 5:00AM
Publication Location:
Article Title: A New Strategy for Reporting Specific Protein Binding Events at Aqueous --Liquid Crystal Interfaces in the Presence of Non-Specific Proteins
Authors: Chul Soon Park, Kazuki Iwabata, Uma Sridhar, Michael Tsuei, Khushboo Singh, Young-Ki Kim, S. Thay
Keywords: self-assembly, interfaces, liquid crystals
Abstract: Aqueous-liquid crystal (LC) interfaces offer promise as respon-sive interfaces at which biomolecular recognition events can be amplified into macroscopic signals. However, the design of LC interfaces that distinguish between specific and non-specific protein interactions remains an unresolved challenge. Herein we report the synthesis of amphiphilic monomers, dimers and trimers conjugated to sulfonamide ligands via triazole rings, their assem-bly at aqueous-LC interfaces, and the orientational response of LCs to the interactions of carbonic anhydrase II (CAII) and serum albumin with the oligomer-decorated LC interfaces. Of six oli-gomers synthesized, only dimers without amide methylation were found to assemble at aqueous interfaces of nematic 4-cyano-4'-pentylbiphenyl (5CB) to induce perpendicular LC orientations. At dimer-decorated LC interfaces, we found that concentrations of CAII less than 4 ?M did not measurably perturb the LC but prevented....
Distribution Statement: 2-Distribution Limited to U.S. Government agencies only; report contains proprietary info
Acknowledged Federal Support: **Y**

RPPR Final Report
as of 06-Jun-2022

Publication Type: Journal Article Peer Reviewed: Y **Publication Status:** 1-Published
Journal: Liquid Crystals
Publication Identifier Type: DOI Publication Identifier: 10.1080/02678292.2019.1662116
Volume: 47 Issue: 4 First Page #: 540
Date Submitted: 8/31/20 12:00AM Date Published: 9/1/19 4:00AM
Publication Location:
Article Title: New room temperature nematogens by cyano tail termination of alkoxy and alkylcyanobiphenyls and their anchoring behavior on metal salt-decorated surface
Authors: Kunlun Wang, Tibor Szilvási, Jake Gold, Huaizhe Yu, Nanqi Bao, Prabin Rai, Manos Mavrikakis,
Keywords: liquid crystals
Abstract: Aqueous-liquid crystal (LC) interfaces offer promise as respon-sive interfaces at which biomolecular recognition events can be amplified into macroscopic signals. However, the design of LC interfaces that distinguish between specific and non-specific protein interactions remains an unresolved challenge. Herein we report the synthesis of amphiphilic monomers, dimers and trimers conjugated to sulfonamide ligands via triazole rings, their assem-bly at aqueous-LC interfaces, and the orientational response of LCs to the interactions of carbonic anhydrase II (CAII) and serum albumin with the oligomer-decorated LC interfaces. Of six oli-gomers synthesized, only dimers without amide methylation were found to assemble at aqueous interfaces of nematic 4-cyano-4'-pentylbiphenyl (5CB) to induce perpendicular LC orientations. At dimer-decorated LC interfaces, we found that concentrations of CAII less than 4 ?M did not measurably perturb the LC but prevented....
Distribution Statement: 2-Distribution Limited to U.S. Government agencies only; report contains proprietary info
Acknowledged Federal Support: **Y**

Publication Type: Journal Article Peer Reviewed: Y **Publication Status:** 1-Published
Journal: Chemistry of Materials
Publication Identifier Type: DOI Publication Identifier: 10.1021/acs.chemmater.0c02415
Volume: 32 Issue: 15 First Page #: 6753
Date Submitted: 8/31/20 12:00AM Date Published: 7/1/20 4:00AM
Publication Location:
Article Title: Self-Assembly of Macromolecules Within Single Topological Defects of Nematic Solvents
Authors: JungHyun Noh, Wei Cao, Hao Sun, Yu Yang, Nathan C. Gianneschi, Nicholas L. Abbott
Keywords: polymers, topological defects, liquid crystals, self-assembly
Abstract: Solvent-mediated self-assembly of macromolecules has been widely used as a bottom-up strategy for synthesis of nanostructured materials, but most solvents (e.g., water or isotropic organic solvents) provide limited control over the spatial localization and ma-nipulation of individual assemblies. In this study, we use organic solvents with nematic ordering to explore the possibility of pro-grammed assembly of polymers with tailored side-chains within the nanoscopic cores of topological defects of the nematic solvents by developing structure-property relationships. Variation of the side chains of poly(n-alkyl acrylates) (alkyl = butyl, hexyl, and do-decyl) revealed that the driving force for partitioning of the polymers into the nanoscopic cores of topological defects formed in ne-matic 4'-n-pentyl-4-biphenylcarbonitrile (5CB) increased with side-chain length, but controlled self-assembly was not observed. Poly(dimethylacrylamide) was found to be soluble in bulk nematic 5CB but did not
Distribution Statement: 2-Distribution Limited to U.S. Government agencies only; report contains proprietary info
Acknowledged Federal Support: **Y**

RPPR Final Report
as of 06-Jun-2022

Publication Type: Journal Article Peer Reviewed: Y **Publication Status:** 1-Published
Journal: The Analyst
Publication Identifier Type: DOI Publication Identifier: 10.1039/D0AN02220A
Volume: 146 Issue: 4 First Page #: 1224
Date Submitted: 5/17/22 12:00AM Date Published:
Publication Location:
Article Title: Using machine learning and liquid crystal droplets to identify and quantify endotoxins from different bacterial species
Authors: Shengli Jiang, JungHyun Noh, Chulsoon Park, Alexander D. Smith, Nicholas L. Abbott, Victor M. Zavala
Keywords: liquid crystals
Abstract: Detection and quantification of bacterial endotoxins is important in a range of health-related contexts, including during pharmaceutical manufacturing of therapeutic proteins and vaccines. Here we combine experimental measurements based on nematic liquid crystalline droplets and machine learning methods to show that it is possible to classify bacterial sources (Escherichia coli, Pseudomonas aeruginosa, Salmonella minnesota) and quantify concentration of endotoxin derived from all three bacterial species present in aqueous solution. The approach uses flow cytometry to quantify, in a high-throughput manner, changes in the internal ordering of micrometer-sized droplets of nematic 4-cyano-4 ' -pentylbiphenyl triggered by the endotoxins. The changes in internal ordering alter the intensities of light side-scattered (SSC, large-angle) and forward-scattered (FSC, small-angle) by the liquid crystal droplets. A convolutional neural network (Endonet) is trained using the large data sets generate
Distribution Statement: 1-Approved for public release; distribution is unlimited.
Acknowledged Federal Support: **Y**

Publication Type: Journal Article Peer Reviewed: Y **Publication Status:** 1-Published
Journal: ACS Applied Materials & Interfaces
Publication Identifier Type: DOI Publication Identifier: 10.1021/acsami.0c11138
Volume: 12 Issue: 37 First Page #: 42099
Date Submitted: 5/17/22 12:00AM Date Published: 8/1/20 4:00AM
Publication Location:
Article Title: Structural and Optical Response of Polymer-Stabilized Blue Phase Liquid Crystal Films to Volatile Organic Compounds
Authors: Yu Yang, Young-Ki Kim, Xin Wang, Michael Tsuei, Nicholas L. Abbott
Keywords: liquid crystals
Abstract: Engineering useful mechanical properties into stimuli-responsive soft materials without compromising their responsiveness is, in many cases, an unresolved challenge. For example, polymer networks formed within blue-phase liquid crystals (BPs) have been shown to form mechanically robust films, but the impact of polymer networks on the response of these soft materials to chemical stimuli has not been explored. Here, we report on the response of polymer-stabilized BPs (PSBPs) to volatile organic compounds (VOCs, using toluene as a model compound) and compare the response to BPs without polymer stabilization and to polymerized nematic and cholesteric phases. We find that PSBPs generate an optical response to toluene vapor (change in reflection intensity under crossed polars) that is sixfold greater in sensitivity than the polymerized nematic or cholesteric phases and with a limit of detection (140 +/- 10 ppm at 25 degrees C) that is relevant to the measurement of permissible exposure limit
Distribution Statement: 1-Approved for public release; distribution is unlimited.
Acknowledged Federal Support: **Y**

RPPR Final Report
as of 06-Jun-2022

Publication Type: Journal Article Peer Reviewed: Y **Publication Status:** 1-Published
Journal: Langmuir
Publication Identifier Type: DOI Publication Identifier: 10.1021/acs.langmuir.9b02975
Volume: 36 Issue: 25 First Page #: 6948
Date Submitted: 5/17/22 12:00AM Date Published: 5/18/20 12:40AM
Publication Location:
Article Title: Steering Active Emulsions with Liquid Crystals
Authors: Karthik Nayani, Ubaldo M. Córdova-Figueroa, Nicholas L. Abbott
Keywords: liquid crystals
Abstract: Colloids dispersed in liquid crystals (LCs) diffuse preferentially along the LC director because this direction of displacement generates the lowest hydrodynamic drag. In this article, we report on the active transport of micrometer-sized nematic droplets of 4'-pentyl-4-biphenyl-carbonitrile (5CB) propelled through a continuous LC phase formed from aqueous solutions of disodium cromoglycate (DSCG) by Marangoni stresses (generated through the addition of sodium dodecyl sulfate (SDS)). We observe the nematic droplets to exhibit motion guided by the continuous LC phase, but in contrast to passive diffusion, the LC droplets move preferentially in a direction perpendicular to the continuous-phase LC director. Our results suggest that the LC droplets, with internal symmetry broken by the Marangoni flow, interact through orientation-dependent van der Waals forces with the LC continuous phase, biasing the orientation of the droplets and the direction of propulsion orthogonal to the far-field d
Distribution Statement: 2-Distribution Limited to U.S. Government agencies only; report contains proprietary info
Acknowledged Federal Support: **Y**

Publication Type: Journal Article Peer Reviewed: Y **Publication Status:** 1-Published
Journal: Advanced Intelligent Systems
Publication Identifier Type: DOI Publication Identifier: 10.1002/aisy.201900114
Volume: 2 Issue: 2 First Page #: 1900114
Date Submitted: 5/17/22 12:00AM Date Published: 1/1/20 3:00PM
Publication Location:
Article Title: Control of the Folding Dynamics of Self?Reconfiguring Magnetic Microbots Using Liquid Crystallinity
Authors: C. Wyatt Shields, Young-Ki Kim, Koohee Han, Andrew C. Murphy, Alexander J. Scott, Nicholas L. Abbo
Keywords: liquid crystals
Abstract: Reconfigurable microdevices are being explored in a range of contexts where their life-like abilities to move and change shape are important. While much work has been done to control the motion of these microdevices by engineering their geometry and composition, little is known about their dynamics in complex fluid environments with non-Newtonian rheology. Herein, it is shown how the actuation dynamics of reconfigurable microdevices made by assembly of patchy magnetic microcubes, which are referred to as "microbots," can be modulated by their interactions with the anisotropic viscoelastic environment of a liquid crystal (LC). The free energy arising from the elastic strain of LC and formation of topological defects around the microbots influences their folding dynamics, which can be tuned by tailoring both the far-field orientation of the LC and the local ordering of the LC at the microbot surfaces. These findings represent a first step toward establishing a general set of design rules
Distribution Statement: 3-Distribution authorized to U.S. Government Agencies and their contractors
Acknowledged Federal Support: **Y**

RPPR Final Report
as of 06-Jun-2022

Publication Type: Journal Article Peer Reviewed: Y **Publication Status:** 1-Published
Journal: Proceedings of the National Academy of Sciences
Publication Identifier Type: DOI Publication Identifier: 10.1073/pnas.2007753117
Volume: 117 Issue: 42 First Page #: 26083
Date Submitted: 5/17/22 12:00AM Date Published: 10/1/20 4:00AM
Publication Location:
Article Title: Dynamic and reversible shape response of red blood cells in synthetic liquid crystals
Authors: Karthik Nayani, Arthur A. Evans, Saverio E. Spagnolie, Nicholas L. Abbott
Keywords: liquid crystals
Abstract: Mammalian cells are soft, and correct functioning requires that cells undergo dynamic shape changes in vivo. Although a range of diseases are associated with stiffening of red blood cells (RBCs; e.g., sickle cell anemia or malaria), the mechanical properties and thus shape responses of cells to complex viscoelastic environments are poorly understood. We use vapor pressure measurements to identify aqueous liquid crystals (LCs) that are in osmotic equilibrium with RBCs and explore mechanical coupling between RBCs and LCs. When transferred from an isotropic aqueous phase into a LC, RBCs exhibit complex yet reversible shape transformations, from initially biconcave disks to elongated and folded geometries with noncircular cross-sections. Importantly, whereas the shapes of RBCs are similar in isotropic fluids, when strained by LC, a large variance in shape response is measured, thus unmasking cell-to-cell variation in mechanical properties. Numerical modeling of LC and cell mechanics reveal

Acknowledged Federal Support: **Y**

Partners

,

I certify that the information in the report is complete and accurate:
Signature: nicholas abbott
Signature Date: 5/17/22 4:54PM

Key Accomplishments

1. **Development of a new experimental system to generated topological defects in liquid crystals.**

A key goal of our project was to develop an understanding of molecular self-assembly of amphiphiles templated from topological defects in liquid crystals. In our past experimental studies, we generated defects by dispersing silica microparticles, treated with octyltrichlorosilane, in an isotropic phase of 4-cyano-4'-pentylbiphenyl (5CB) that contained a predetermined concentration of amphiphile (BODIPY-C5). The surface treatment of the microparticles promoted perpendicular anchoring of the nematic liquid crystals. The particle-liquid crystal mixture was introduced in the isotropic state between two glass substrates that were polyimide-coated, unidirectionally rubbed, and oriented 90° relative to one another, thereby inducing twist within the nematic phase upon cooling (**Fig. 1**). In the presence of the surface-treated particles, the combined boundary conditions yield a singular line defect of strength -1/2 around and between the particles. This procedure readily produces line defects, but limits the long-term study of defects because the lengths of the defect lines change over time as particles migrate in the liquid crystal medium. Typically, the distance between particles shortens over time to reduce the lengths of the defects and minimize the free energy of the system. This relaxation of the defects over time made quantitative characterization of self-assembly of molecules within the defects challenging and motivated efforts pursued over the past year to generate better defined defects.

To address the above-described limitation of our prior experimental approach, as part of our project, we developed a new system for studying self-assembly in topological defects. As shown in **Fig. 1b**, two metallic wires were introduced between two planar glass substrates. Both the wires and the glass substrates were treated with dimethyloctadecyl[3-(trimethoxysilyl)propyl]ammonium (DMOAP) to induce perpendicular anchoring of nematic liquid crystals at their surfaces. These boundary conditions cause the director field of the liquid crystal to bend and generate two line defects of strength -1/2, satisfying the topology of the confined nematic domain. As drawn in **Fig. 1b**, the director is locked perpendicular to the two glass substrates, while the director bends upon approaching the wires. The resulting defect lines run parallel to the surfaces of the wires, as shown by the red defect (disclination) cores in Fig 1b. Since the boundary condition is defined by stationary elements, we found that the new system reliably creates -1/2 disclinations, avoiding issues associated with microparticles freely dispersed

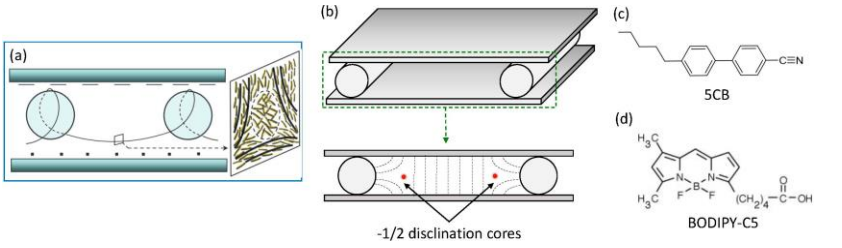

Figure 1. Experimental designs and materials. (a) The original design for generating a -1/2 line defect (disclination) by adding microparticles to a nematic liquid crystal. (b) New experimental design of optical cells for creating -1/2 disclinations that are running parallel to the wires. (c-d) Molecular structures of compounds; (c) a nematic liquid crystal (5CB) and (d) dipyrromethene borondifluoride (BODIPY)-labelled amphiphile.

in liquid crystals in our previous setup. Additionally, we confirmed that the generated disclinations were stable over three weeks.

Using the above-described system, we performed measurements of self-assembly in topological defects of 5CB (**Fig. 2**). The experimental procedure involved introducing an isotropic mixture of 5CB and BODIPY-C5 into the newly designed optical cell. As the mixture was cooled to the nematic phase, the boundary conditions cause singular disclinations to be formed approximately 30-40 μm from the surface of the wires (for 300 μm-diameter wires). As noted above, the direction of the disclinations (defect lines) is parallel to the long axes of the wires. The line defects are millimeters in length and both ends anchor on the wire surface. Optical microscopy can readily image the defects because the core of the defects scatter light (**Fig. 2b**) and because the orientation of the liquid crystals varies abruptly in close proximity to each defect core.

We imaged fluorescently-labeled (i.e., BODIPY-labeled) amphiphiles to observe their self-association behavior in defects. The fluorescence emission of the BODIPY group changes depending on whether it is singly dispersed or self-assembled; measurement of fluorescent emissions using $\lambda^{excitation}$= 533-584 nm *and* $\lambda^{emission}$ = 606-684 nm indicates self-association of the amphiphiles. When using 70 μM BODIPY-C5 in 5CB, fluorescence microscopy (**Fig. 2c**) revealed that the amphiphiles are assembled in the defect (intense fluorescence along the disclination). This result suggests that the critical aggregation concentration of the BODIPY-C5 is less than 70 μM in the environment of the -1/2 defect. Overall, however, measurements such as these have established the feasibility of using this new experimental system for studies of self-assembly in defects. This experimental geometry was used extensively in the additional studies performed in this project, as reported below.

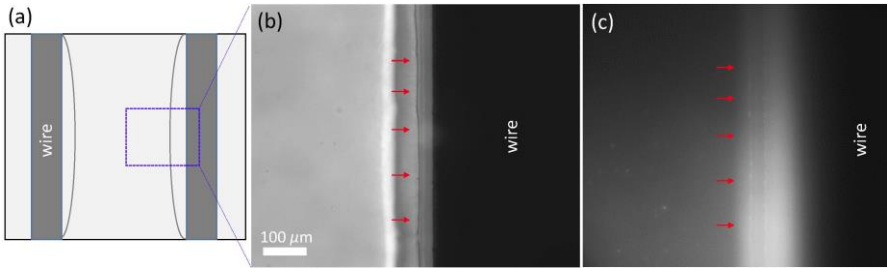

Figure 2. Disclination lines and self-assembly of amphiphiles in a line defect. (a) Schematic illustration of two -1/2 line defects generated by the boundary conditions and anchored on the wires. (b) Optical micrograph of a line defect (indicated by red arrows) and (c) Fluorescence micrograph ($\lambda^{excitation}$ 533-584 nm , $\lambda^{emission}$ 606-684 nm) showing the selectively assembled amphiphiles in the disclination through the intense fluorescence (indicated by red arrows).

2. Development of Structure-Property Relationships for Polymers in Topological Defects of Liquid Crystals.

A second key goal of our project was to study the self-assembly of polymers in defects in liquid crystals. To this end, we employed RAFT to synthesize a range of homopolymers labelled with the fluorophore BODIPY, as shown in **Figure 3,** to develop structure-property relationships for self-assembly in defects. BODIPY was chosen as the fluorophore because the absorption and emission spectra of BODIPY changes with self-association, thus providing an unambiguous optical signature of the onset of self-association of the homopolymers in 5CB. When BODIPY

is singly dispersed in nematic 5CB, absorption and emission occur at 457-502 nm and 510-562 nm, respectively, while association of the fluorophore into dimers results in absorption and emission at 533-584 nm and 606-684 nm, respectively.

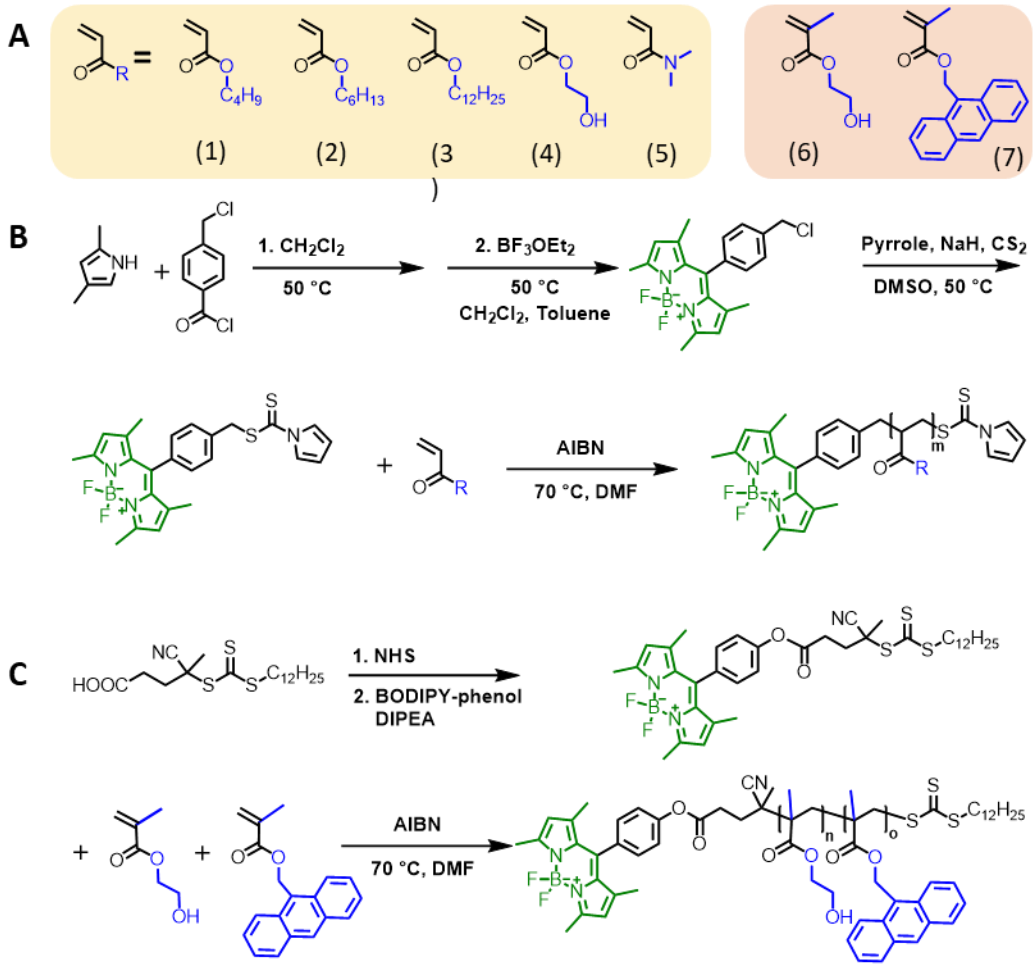

Figure 3. Molecular structures of monomers and synthetic pathways for the preparation of BODIPY-conjugated homopolymers. (**A**) Chemical structures of monomers, containing acrylate or acrylamide (highlighted in yellow box) and methacrylates (red box); **(1)** butyl acrylate, C4; **(2)** hexyl acrylate; C6; **(3)** dodecyl acrylate, C12; **(4)** 2-hydroxylethyl acrylate, HEA; **(5)** dimethylacrylamide, DMA; **(6)** 2-hydroxyethyl methacrylate, HEMA; **(7)** 9-anthracenylmethyl methacrylate, AnMA. (**B-C**) Synthesis of polyacrylate and polyacrylamide **(B)** and (**C**) polymethacrylate via RAFT polymerization. BODIPY fluorophore is highlighted in green. NHS, N-Hydroxysuccinimide; DIPEA, N,N-Diisopropylethylamine.

We synthesized BODIPY-labelled dithiocarbamate CTA in two steps as described in Figure 4.

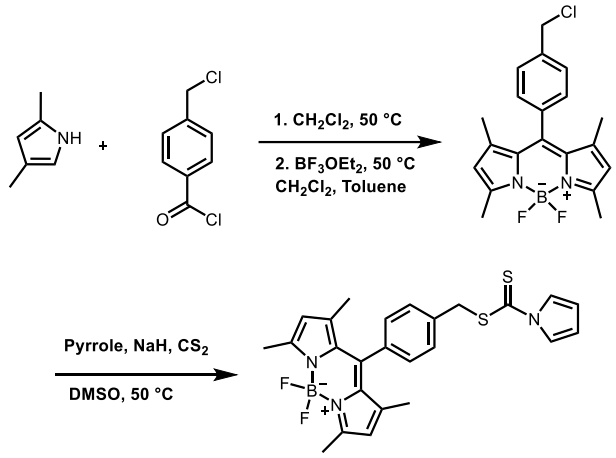

Figure 4. Synthetic route for BODIPY-CTA 1.

To match the reactivity of methacrylate monomers, a trithiocarbonate CTA (BODIPY-CTA 2) was synthesized by esterification of a phenol BODIPY with a -COOH bearing trithiolcarbonate (Figure 5).

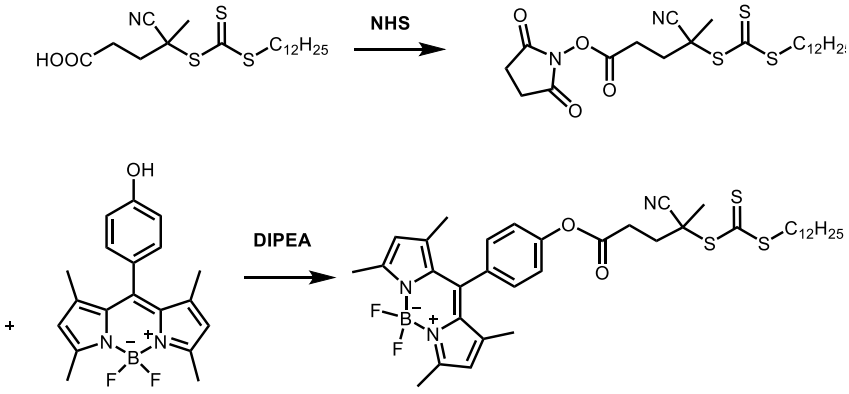

Figure 5. Synthetic route of trithiocarbonate BODIPY-CTA 2.

RAFT (reversible addition fragmentation transfer) polymerization was performed in DMF with AIBN as the initiator. Non-polar polymers synthesized include C4, C6 and C12 and polar polymers include HEMA, HEA and DMA. Cross-linkable polymers were made by copolymerization methods. Detailed are summarized in **Figures 6 and 7**.

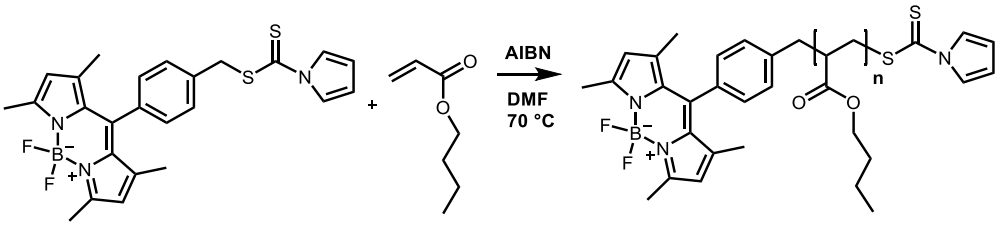

Figure 6. Synthetic route for BODIPY-poly(C4).

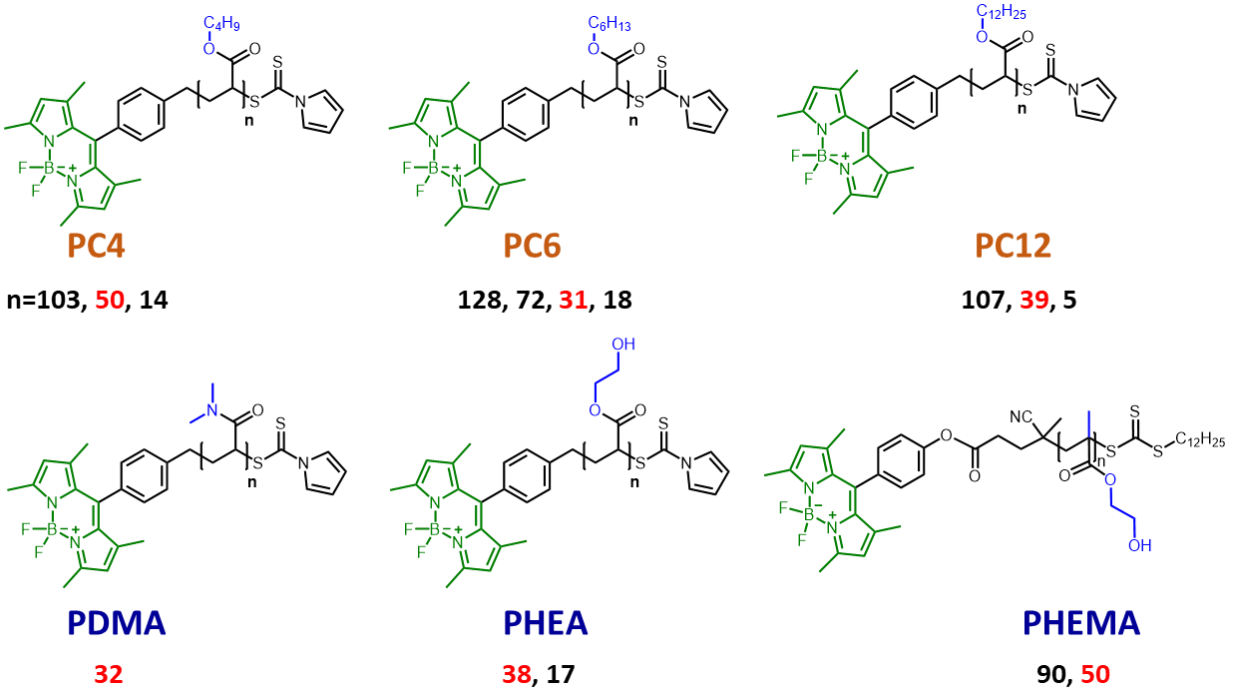

Figure 7. BODIPY labelled polymer structures. Including PC4, PC6, PC12, PDMA, PHEA and PHEMA.

Table 1. Polymers synthesized.

Polymer type	Identifier[a]	DP_m[b]	DP_n[b]	DP_o[b]	$M_{n,NMR}$ (g/mol)	$M_{n,GPC}$ (g/mol)	PDI[c]
Homopolymers	C4	103			13.8k	12.9k	1.17
	C4	50			6.9k	9.0k	1.25
	C4	14			2.3k	N/A	N/A
	C6	72			11k	9.2k	1.37
	C6	18			3.3k	2.1k	1.36
	C12	107			26.2k	18.0k	1.47
	C12	39			9.8k	4.8k	1.34
	C12	5			1.7k	N/A	N/A
	HEA	38			4.9k	12.5k	1.32
	DMA	32			3.7k	7.6k	1.32
	HEMA		90		12.0k	24.5k	1.33
	HEMA		50		7.2k	27k	1.30
Random copolymers	HEMA-*r*-AnMA		46	18	11.7k	26.8k	1.38
	HEMA-*r*-AnMA		22	23	9.9k	13.4k	1.54

[a]Structures of R groups are shown in **Figure 6 and 7**. [b]Degree of polymerization (DP) for each monomer is indicated by *m*, *n* or *o*, as determined by NMR and GPC. [c]Polydispersity index (PDI) determined by GPC is indicated for each polymer. For N/A, the retention time is too long to calculate M_n and PDI by GPC.

We performed extensive studies of the self-assembly of the polymers described above in bulk liquid crystalline solvents and in topological defects. While our focus was directed to self-assembly in defects of LCs, it was also important to understand the behaviors of the polymers in the bulk LC. In this respect, the generalization described in the published literature is that flexible polymers have low solubilities in nematic solvents because the structure of the solvent constrains configurational degrees of freedom. This generalization was consistent with observations related to a number of the polymers in Table 1, however, a striking departure from it was the behavior of poly(DMA). Here we illustrate our finding with poly(DMA) by comparing its behavior to poly(HEA).

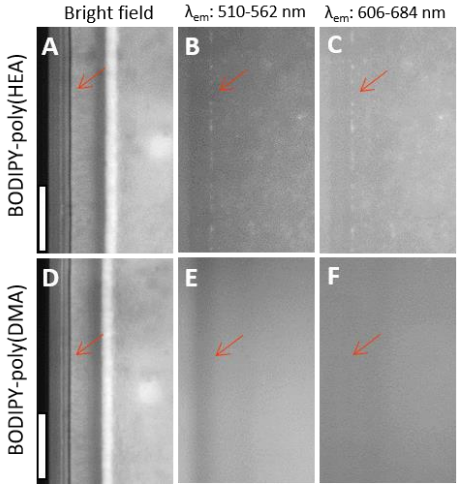

Figure 8. (A-C) Aggregation of BODIPY-poly(HEA) (DP = 38) at 1 μM in nematic 5CB. (D-F) Dissolution of BODIPY-poly(DMA) (DP = 32) at 1 μM in nematic 5CB. (A, D) Bright field and (B-C, E-F) fluorescence micrographs; (B, E) with monomeric (λem = 510-562 nm) and (C, F) dimeric signals (λem = 606-684 nm), showing the distribution of polymers in the nematic 5CB. Red arrows indicate the locations of defects. Scale bars are 100 μm.

Inspection of **Figure 8A-C** reveals that BODIPY-poly(HEA) (DP = 38) at 1 μM in nematic 5CB forms aggregates, consistent with its low solubility. We compared this behavior to BODIPY-poly(DMA) with DP = 32 (**Figure 1D-F** and Table 1). The amide group of BODIPY-poly(DMA) possesses a large dipole moment (e.g. dimethylacetamide, 3.79 D). We found this polymer to exhibit exceptionally high solubility in nematic solvents compared to the other polymers used in our study. At concentrations up to 200 μM, we detected no sign of aggregation of the polymer in defects or bulk LC (no dimer signal); the monomer fluorescent signal intensity increased monotonically over the concentration range studied. These results suggest that the amide group of BODIPY-poly(DMA) interacts favorably with 5CB in the nematic phase. *This result is important because it reveals that poly(DMA) is a privileged block with high solubility in nematic 5CB and that it has the potential to be used as a solvophilic block in polymer self-assembly processes in nematic solvents.*

We found that BODIPY-poly(HEMA) exhibited all the thermodynamic signatures of self-assembly in $-1/2$ topological defects of nematic 5CB. To provide insight into the nanostructure of BODIPY-poly(HEMA) assemblies formed in $-1/2$ defects of 5CB, we formed assemblies from related polymers with side chains that can be photo-crosslinked, and then extract and characterize the assemblies post-crosslinking. Specifically, we synthesized the random copolymer BODIPY-poly(HEMA-r-AnMA) that incorporated the anthracenyl monomer, AnMA (Table 1). We chose AnMA to match the reactivity of HEMA, a methacrylate, and to provide side chains that can be cross-linked by UV exposure. Past studies have shown that anthracene will undergo a [4π+4π] cycloaddition upon UV exposure. We confirmed the photodimerization of anthracene in BODIPY-poly(HEMA-r-AnMA) by monitoring the decrease of the $\pi-\pi^*$ absorption at 368 nm in DMF using UV-Vis spectroscopy.

We found that BODIPY-poly(HEMA46-r-AnMA18), (where the subscripted number indicates DP of a monomer incorporated into the polymer (randomly)) selectively self-assembled within $-1/2$ defects of 5CB above a critical aggregation concentration (CAC). However, the presence of the anthracenyl monomer within the copolymer was observed to cause the CAC of the polymer to increase relative to BODIPY-poly(HEMA) of comparable DP. For example, the CAC of poly(HEMA46-r-AnMA18) was measured to be 0.45 ± 0.05 μM (Table 1), which is 2.5 time higher than that of BODIPY-poly(HEMA) with DP = 50 (0.25 ± 0.05 μM). In addition, when the ratio of HEMA and AnMA was 1:1 with BODIPY-poly(HEMA22-r-AnMA23), we did not observe self-assembly up to a concentration of 1 μM. Above 1.5 μM, we observed aggregates to form in bulk LC with sizes of tens of micrometers, indicating that the solubility limit of the polymer was exceeded in the bulk LC solvent.

Guided by the results above, we assembled BODIPY-poly(HEMA46-r-AnMA18) in LC defects (confirmed by fluorescence signature), exposed the defect to UV light, and then heated the nematic solvent above the clearing temperature to eliminate the defect. When the defect was eliminated by heating to 40°C, the cross-linked assembly did not fragment but rather a contiguous structure was observed to be suspended in isotropic 5CB (**Figure 9A**). This result contrasts to other experiments where the assembly of BODIPY-poly(HEMA) fragmented then dissolved upon heating of the 5CB from the nematic to isotropic phase.

To transfer the cross-linked polymeric assembly from the isotropic 5CB phase (Figure 9A) to the surface of a solid for SEM and AFM, we used a pipette to withdraw the isotropic 5CB containing the cross-linked assembly from the optical cell and deposit it onto the surface of a glass microscope slide. Adoption of this procedure was guided by the observation that the polymeric assemblies adsorbed to the surface of the microscope slide. While we were able to use fluorescence imaging (acquisition times of about 2 seconds) to observe assemblies of BODIPY-poly(HEMA46-r-AnMA18) form within LC defects at

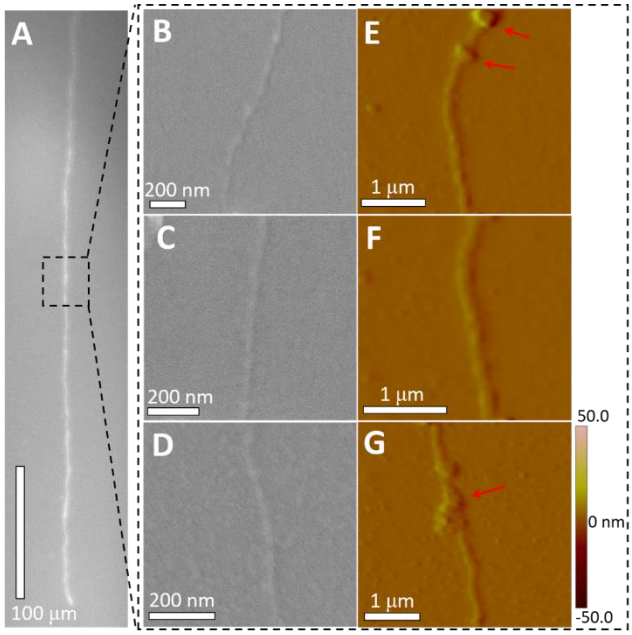

Figure 9. Structure of assemblies of BODIPY-poly(HEMA46-r-AnMA18) formed in $m = -1/2$ topological defects of 5CB and preserved by photo-crosslinking. The concentration of polymer in the 5CB sample was 0.7 µM. (A) Fluorescence micrograph of a cross-linked assembly suspended in isotropic 5CB. (B-D) Representative SEM and (E-G) AFM images of cross-linked assemblies of BODIPY-poly(HEMA46-r-AnMA18) transferred to the surface of glass substrates. Red arrows point to aggregates formed in bulk nematic 5CB that attach to the nanofiber, and were used to identify the locations of the nanofibers on the glass substrates (see text for details).

concentrations of the polymer of ~0.5 µM, after transfer of the assembly to the surface of the microscope slide, we were no longer able to localize the assembly by fluorescence imaging (even by using long acquisition time). However, by using higher concentrations of BODIPY-poly(HEMA46-r-AnMA18), specifically concentrations above which aggregation of the polymer also occurred in the bulk 5CB, we found that attachment of bulk aggregates to the polymeric assembly formed in the defect provided an effective and simple method to identify the location of the defect-templated assembly on the glass microscope slide for imaging by SEM and AFM.

Both imaging methods led to identification of worm-like polymeric assemblies that had lengths greater than 10 µm (Figure 9B-G). As noted above, the worm-like assembly, which was readily identified due to its uniformity in width, was decorated by disordered polymer aggregates that formed in the bulk of the LC and attached to the assembly formed in the defect. In many images, we observed the defect-templated polymeric assembly to pass under, and extend for 10's of micrometers on either side of the aggregates formed in the bulk LC (Figure 9). We characterized the widths of the defect-templated polymeric assemblies using three independent samples. We measured the widths at multiple places along each assembly by SEM and calculated the mean and standard deviations to be 33 ± 3 nm, 30 ± 6 nm, and 27 ± 3 nm, respectively. The uniformity in the thicknesses of the nanofibers is consistent with controlled growth of the assemblies within

the defects. We also used AFM to characterize the nanofibers (same samples used to SEM). While AFM confirmed the uniformity of width, convolution of the AFM tip shape with the nanofiber leads to an overestimate of the nanofiber diameters (the apparent diameters measured by AFM were 136 ± 19 nm, 148 ± 29 nm, and 123 ± 10 nm, respectively). The radius of curvature of the AFM tip used in our study was 30 nm, which is larger than radius of nanofiber (radius of 15 nm, as determined by SEM). We calculated that convolution of the AFM tip shape (radius of 30 nm) with the topography of the nanofiber (diameter of 30 nm) to generate an apparent nanofiber diameter of 120 nm, which is in good agreement with the average of the above-reported experimentally determined values (135 nm ± 20 nm). Overall, the result represents the first characterization of the nanostructure of a polymeric assembly formed within the defect of a LC. Specifically, it established that it is possible to form well-defined nanostructures with uniform dimensions, consistent with a nanostructure controlled by a self-assembly process. Our future experiments will explore the effects of polymer architecture on the morphology of assemblies formed within defects. Todate, we have observed worm-like assemblies to form, but we predict, similar to bulk self-assembly of polymers, a range of other morphologies should be accessible via control of architecture.

4. **Influence of molecular self-assembly on defect dynamics in liquid crystals**

One of the key goals of our project was to understand how molecular self-assembly influences the dynamics of defect motion, with the ultimate goal of showing how macroscopic dynamics of defects can be harnessed to report formation of a single nanoscopic amphiphilic assembly. As detailed in our proposal, our initial experiments were based on generating ±1 point defects by heating 5CB into an isotropic phase and subsequently wicking it into capillaries with inner diameter (DO) of 400 μm. The inner surfaces of the capillaries were chemically-functionalized with N,N-dimethyl-N-octadecyl-3-aminopropyl-trimethoxysilyl chloride (DMOAP) to induce perpendicular (homeotropic) anchoring of the LC director. Following filling of the capillary, the 5CB was quenched thermally into the nematic phase. This geometry results in point singularities that can be observed optically along the capillary axis at domain boundaries. The ±1 defects are attracted to each other due to the elasticity of the liquid crystal (**Fig 10a-f**). This attractive interaction acts on both defects with opposite strengths over a very large separation (several hundreds of micrometers). At separations lower than tens of micrometers, we observed the defects to optically fuse limited by optical resolution. After contacting with each other, they annihilate, resulting in a defect-free liquid crystal ordering. Fluorescence micrographs in Figs. 1g show that the molecular assemblies remain intact immediately after defect annihilation. Over the subsequent 30 min, the assemblies (of DLPC) slowly dissociated and diffused in the defect-free nematic LC, indicating that these molecular assemblies are long-lived. Representative TEM micrograph of the molecular assemblies shows toroidal-shape assemblies comprised of three periodic lipid bilayers, as shown in **Fig. 10h**. This observation is consistent with previous theoretical studies that predicted the core structure of +1 defects to be nanoscopic closed-loop disclination.

To provide insight into the role of the molecular assemblies in defining the dynamics of defects, we derived a simple model to analyze the dynamics of defects and we tested this model to see if changes in the sizes of assemblies formed within defects are reflected in the changes in the macroscopic dynamics of defects. To set up the model, we evaluated the elastic force driving the defects to annihilate as

$$f_{\text{defect}} = K\left(\frac{d}{D_O}\right)^{-2.9}$$

in which K is the elastic constant of the LC (using the 'one constant' approximation). This elastic force is opposed by a Stokes drag force, which can be written as:

$$f_{\text{drag}} = C_D v$$

in which CD is the Stokes drag coefficient, i.e.,

$$C_D = 6\pi\mu_{\text{apparent}} a$$

where μ_{apparent} is the apparent viscosity, and a is the effective hydrodynamic radius of the topological defects. By interpreting measurements of defect dynamics in terms of a drag coefficient or effective size (a), we have examined how cross-linking of assemblies within defects (i.e., quenching of assembly dynamics) as well as assembly size impact defect dynamics. These experiments were performed using the photoreactive lipid diyne PC doped with 3 % BODIPY-C5 (instead of DLPC). We found that the dynamics of ±1 defects with 5CB/diyne PC mixture are similar to DLPC, with CAC and CSat of diyne PC ~ 10 μM and 19 μM, respectively (see **Fig. 11a**). More importantly, crosslinking of assemblies of diyne PC neither prevented defect annihilation nor changed the dynamics of defects. This observation indicates that the internal dynamics of assemblies within the defect core do not have a significant impact on the dynamics of defects. Furthermore, based on C_D shown in **Fig. 11b,** we calculate the ratio of $a_{19\mu M}^{+1,\,C_D}/a_{10\mu M}^{+1,\,C_D}$ to be ~ 1.34 (i.e., that the assemblies formed from 19 uM lipid are larger than 10 uM lipid, by a factor to 1.34). To test this prediction based on defect dynamics, we measured independently the Brownian motion of self-assembled core in nematic 5CB with uniform homeotropic alignment, as shown in **Fig. 11c**. Fig. 10 shows the mean square displacement (MSD) as a function of time. The diffusion coefficient D can be calculated from the MSD. Based on the MSDs and D calculated from **Fig. 11d**, we

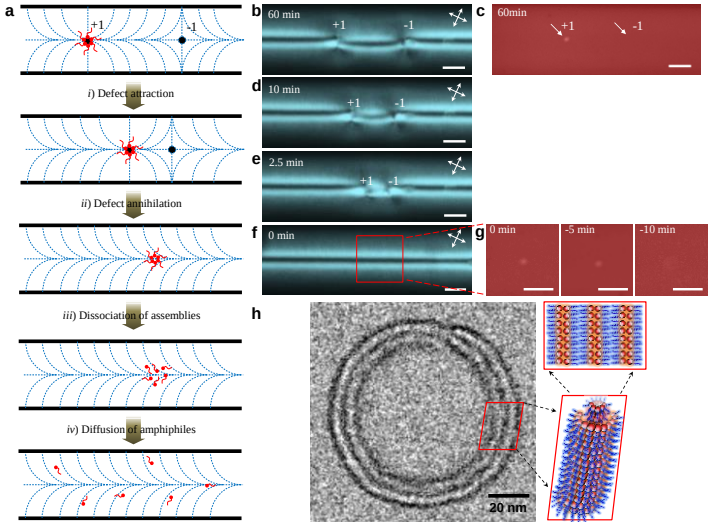

Figure 10. Dynamics of defects and self-assembled defect cores. a, Schematic illustration of motion and annihilation of ±1 defects and dynamics of self-assembled defect core in a capillary filled with nematic LC. Dashed blue line illustrates local ordering of mesogens. **b,d-f**, Polarized light micrographs showing the dynamics of defects formed in a mixture of DLPC/5CB in a capillary. The white double-headed arrows indicate the orientation of the crossed polarizers. **c,g**, Fluorescence micrographs showing the temporal evolution of molecular assemblies in this process. DLPC concentration is 57 μM. DLPC is mixed with BODIPY-C5 at 4% mol/mol based on DLPC. The times at which the micrographs were obtained (**b-f**) before or (**g**) after defect annihilation are indicated (time was set to 0 when the defects were annihilated). Scale bars, 100 μm. **h**, Representative TEM image and schematic illustration of diyne PC assemblies templated by +1 defects. Diyne PC concentration is 19 μM

calculate $a_{19\mu M}^{+1,\,MSD}$ = 56 ± 5 nm and $a_{10\mu M}^{+1,\,MSD}$ = 42 ± 4 nm, and thus $a_{19\mu M}^{+1,\,MSD}/a_{10\mu M}^{+1,\,MSD}$ ~1.33, in close agreement with $a_{19\mu M}^{+1,\,C_D}/a_{10\mu M}^{+1,\,C_D}$~1.34. Furthermore, the TEM images of diyne PC assemblies shown in insets in Fig. **10d** lead us to calculate that $a_{19\mu M}^{+1,\,TEM}$ = 65 ± 5 nm, $a_{10\mu M}^{+1,\,TEM}$ = 50 ± 5 nm, and $a_{19\mu M}^{+1,\,TEM}/a_{10\mu M}^{+1,\,TEM}$ ~ 1.30. We note here that $a^{+1,\,TEM}$ is the hydrodynamic size rather than structural size. Overall, these results support our hypothesis that the molecular assemblies expand a^{+1} to slow v^{+1}. The results provide further evidence that measurements of the macroscopic motion of defects can provide insights into changes in the organization of nanoscopic assemblies that form within them. Whereas our previous measurements had shown the formation of assemblies slows defect motion, the key finding in **Fig. 11** is that changes in the sizes of amphiphilic assemblies can also be transduced by measurements of defect motions.

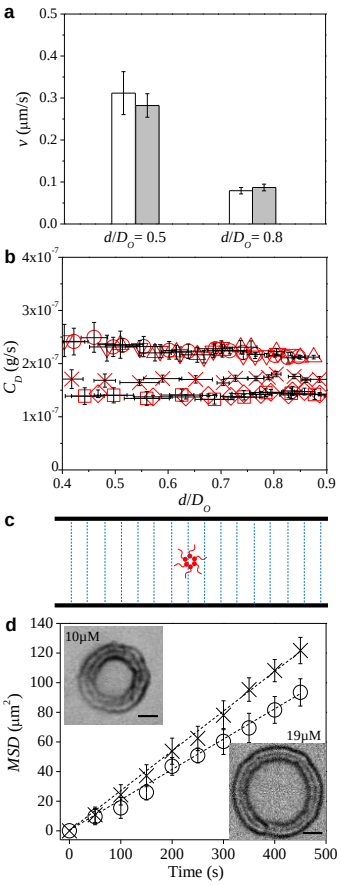

Figure 11 Dynamics of defects in diyne PC/5CB mixture and nanostructure of self-assembled cores. a, v^{+1} of (gray) uncrosslinked and (white) crosslinked self-assembled cores. **b**, C_D of +1 defects as a function of *d*. Pure 5CB: □. Diyne PC: ◇ 5 μM; × 10 μM; ○ 19 μM; Δ 19 μM (crosslinked); ▽ 38 μM. **c**, Scheme of assemblies in homeotropic anchoring LCs. Dashed blue line illustrates local ordering of mesogens. **d**, *MSD* of diffusion of crosslinked self-assembled cores as a function of time. × 10 μM; ○ 19 μM. Dashed lines represent the best-fit of the data. Insets in (**d**) show representative TEM images of diyne PC assemblies templated by +1 defects. Three assemblies at each concentration were characterized. Error bars represent standard deviations and n = 3 for each data point. Scale bars, 20 nm.

5. Electric Field-Induced Transport of Self-assembled Structures using Topological Defects Hosted in Nematic Liquid Crystals: Manipulation of Single Assemblies and Studies of Dynamics

The formation of polymeric assemblies in topological defects, as demonstrated for the first time in this grant from the ARO, is an exciting capability because topological defects can be manipulated and driven into motion using a variety of external fields. This opens up the possibility of establishing fundamentally new ways to transport and position functional assemblies and to study the dynamical properties of molecular assemblies. One approach that we explored for manipulation of defects is the use of electric fields. *As detailed below, we*

found that we can reversibly manipulate the positions of defects with electric fields and that it is possible to transport molecular assemblies with the defects as they are repositioned.

Figure 12 shows the experimental set up that we used to manipulate -1/2 line defects using wire-shaped electrodes (orange cylinders in Figure 12). As described above, in the absence of the electric field, the two line defects formed in the LC equilibrate to positions that are close to the surfaces of the electrode. However, upon application of a potential difference of 25 V between the electrodes, the defects can be seen to move towards the regions of the LC located between the electrodes (i.e., in the direction of the electric fields). The positions of the defects could be manipulated by controlling the applied voltage difference, and they could be moved reversibly between different locations within the LC.

In a second set of experiments, we explored how the presence of molecular assemblies within the defects influences the dynamics of motion of the defects in the presence of the electric field. Inspection of **Figure 13** reveals that the presence of molecular assemblies (formed from fatty acids labeled with BODIPY) within the defects slows the dynamics of defect motion. The slowing of defect motion occurred not only during the application of the electric field but also during relaxation of the defect position after removal of the field. These observations suggest that the presence of the molecular assembly creates "drag" which slows the motion of the defect. Additionally, we observed that the concentration of the BODIPY-C5 present in the LC, which we know from prior studies to impact the size of the nanoscopic assembly formed in the defect, slows the defect dynamics. Specifically, an increase in concentration of the amphiphile leads to a decrease in the defect motion, consistent with an increase in drag created by a larger assembly hosted in the defect.

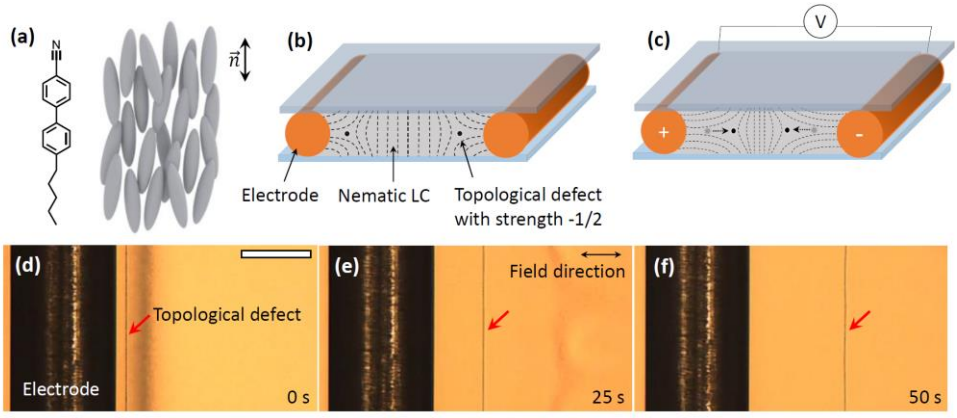

Figure 12: Electric field-induced motion of defects in nematic LCs (a) Chemical structure of 5CB and schematic of a nematic LC with director, $\vec{n}$. (b-c) Experimental set-up used to generate a pair of topological defects with strength m = -1/2 in nematic 5CB in (b) and to move the defects using electric fields in (c). (d-e) Optical

micrographs show a defect moving away from electrode. Time indicates the time after electric field was applied. Scale bar, 200 μm.

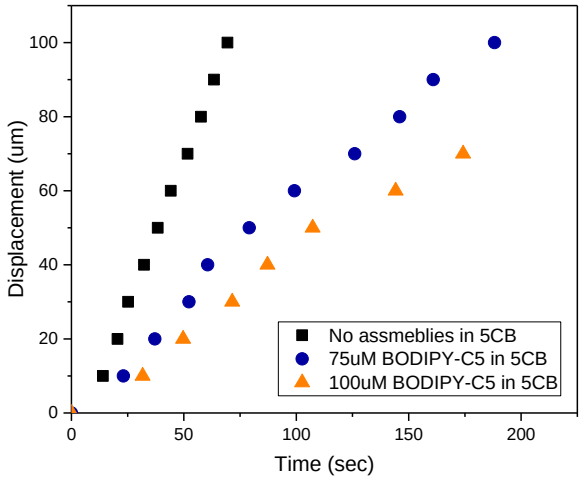

Figure 13: Defect speeds, with and without molecular assemblies, drive by application of an electric field. The speed of defect without loads about 1.6 um/s (at 25V, 1kHz AC).

In addition to showing that defect dynamics are impacted by the hosting of molecular assemblies within a defect, we performed experiments to determine if the fluorescence signature associated with the assembly within the defect "traveled" with the defect as it was driven into motion. These experiments are shown in **Figure 14 and 15**. In **Figure 14**, we used a fatty acid that was labeled with BODIPY, which we have shown previously to assembly in defects. Inspection of **Figure 14** (right side) clearly shows that a peak in fluorescence travels laterally across the sample upon application of the electric field. By using multiple imaging modalities, we confirmed that the peak in fluorescence intensity coincided with the location of the defect. Additionally, we performed experiments with polymeric assemblies within defects, as shown in **Figure 15**. Specifically, we used BODIPY-poly(HEMA) to form a polymeric assembly in a -1/2 defect, and then drove the defect across the sample using an applied electric field. We observed the fluorescence maximum corresponding to the presence of the assembly to move with relocation of the defect upon application of the electric field.

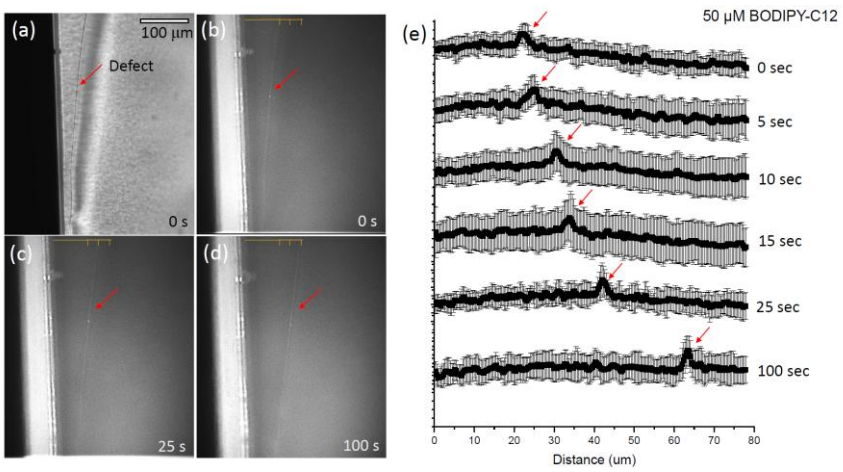

Figure 14: Electric field-driven motion of defects in LC that host assemblies of BODIPY-C12. (a) is a bright field micrograph shown initial location of defect near electrode surface. (c) through (d) are fluorescence micrographs shown location of the "line" corresponding to the assembly of BODIPY-C12 hosted in the defect. (e) shows the location of the defect (indicated by arrow) as a function of time following application of the electric field.

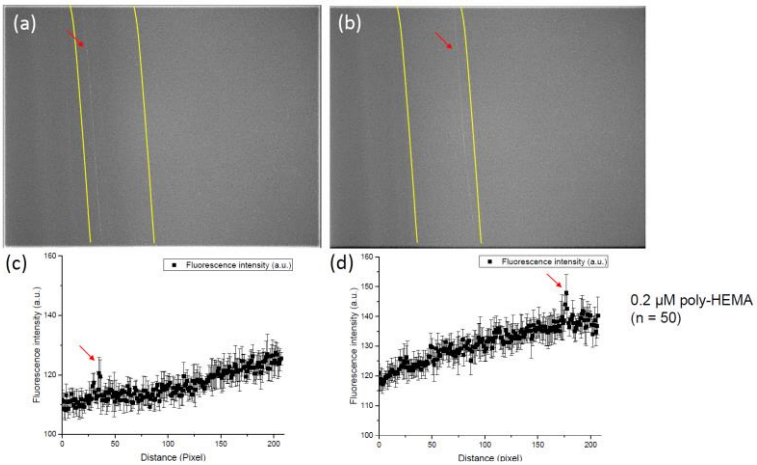

Figure 15: Electric field-driven motion of defects in LC that host assemblies of BODIPY-poly(HEMA). (a) and (b) are fluorescence micrographs shown location of the "line" corresponding to the assembly of BODIPY-poly(HEMA) hosted in the defect. (c and d) show the location of the defect (indicated by arrow) as a function of time following application of the electric field.

The results in **Figures 14 and 15** provide exciting evidence of the possibility of using electric fields to manipulate nanoscopic assemblies formed from either small molecules or polymers within defects. Specifically, we observed the maximum in fluorescence intensity to relocate to the position of the defect, when the defect was moved by application of an electric field. This observation generates and enables studies of a range of interesting questions related to assembly dynamics. It also opens the possibility of moving defects to regions of LCs that contain different self-assembling species, and assembling or disassembling the molecules in defects depending on

defect environment. To provide a first demonstration of this possibility, we formed defects in a LC sample that contained a gradient in concentration of BODIPY-C12. The experimental set-up used to create the gradient in concentration is shown in **Figure 16**. Initially, we introduced a high BODIPY-C12 concentration in the region where the defect is located (green region in **Figure 16**), and then we use the electric field to displace the defect to a region of the sample where the BODIPY-C12 is absence from the bulk LC phase. **Figure 17** shows the result of this experiment. In particular, inspection of the right side panel of the figure shows that the local maximum in fluorescence intensity (highlighted in red color) corresponds to the location of the defect. Interestingly, as the defect is moved from the LC region containing a high concentration of BODIPY-C12 to a region containing a low concentration, the assembly within the defect disassembles. Upon returning the defect to the region of high BODIPY concentration, we observed the fluorescence signature of the assembly within the defect to reform. This exciting result is the first demonstration of control over the assembly and disassembly of molecules with defects by controlling the location of the defect using an electric field. In contrast to BODIPY-C12, which evidently has fast assembly/disassembly dynamics on the timescale of the experiment shown in **Figure 17**. We also characterized the assembly and disassembly processes using the polymers in Table 1. We found the dynamics of the disassembly process involving these polymers to be orders of magnitude smaller, which manifested in long-lived fluorescence of defects that are driven by electric fields into regions of LC free of polymer. Overall, the results above are highly significant as they point the way towards the use of topological defects as nanoscopic reactors that can host both chemical and physical transformations, and be readily manipulated to add and remove reagents.

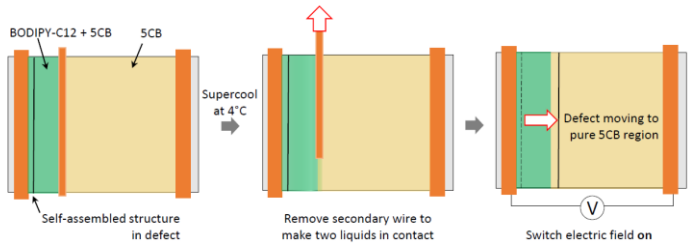

Figure 16: Experimental set-up used to observe spontaneous disassembly of BODIPY-C12 in LC defects. The left panel shows the defect containing an assembly of BODIPY-C12, which was moved toward the amphiphile depletion zone (the bulk concentration is lower than CAC) leading to dissociation of the self-assembled structure in the nematic solvent (right panel).

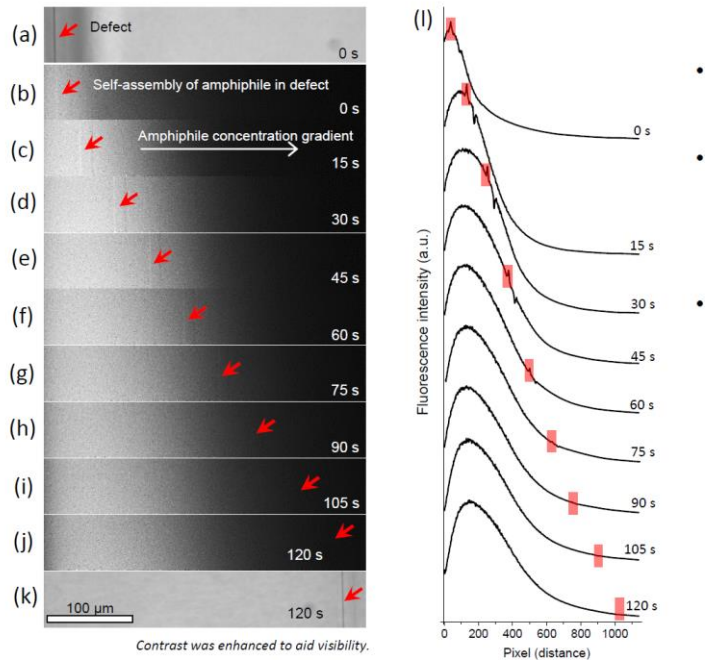

Figure 17: Spontaneous disassembly of an assembly of BODIPY-C12 in a LC defect that is triggered by moving the defect using an electric field. (a, k) Bright field micrographs showing the location of a topological defect (m = -1/2) in a nematic LC. (b-j) Fluorescence micrographs showing dimer fluorescence moving with the defect as a function of time under electric field. Time indicates the time after electric field was applied.(l) Fluorescence intensity measured and averaged in regions (380 µm × 180 µm) within the sample as a function of time. Abrupt increases in dimer fluorescence (indicated by red area) identify the location of self-assembly in the nematic 5CB.The fluorescence signal gradually decreased as the defects loaded with self-assembly of small amphiphiles (BODIPY-C12) moved to the amphiphilic depleted area. Above 75 s, the dimer signal diminished.